

# NMR and Mutagenesis Studies on the Phosphorylation Region of Human Cardiac Troponin I<sup>†</sup>

Douglas G. Ward, Susan M. Brewer, Clare E. Gallon, Yuan Gao, Barry A. Levine, and Ian P. Trayer\*

*School of Biosciences, University of Birmingham, Edgbaston, Birmingham B15 2TT, United Kingdom*

*Received December 23, 2003; Revised Manuscript Received March 5, 2004*

**ABSTRACT:** Phosphorylation of the cardiac troponin complex by PKA at S22 and S23 of troponin I (TnI) accelerates  $\text{Ca}^{2+}$  release from troponin C (TnC). The region of TnI around the bisphosphorylation site binds to, and stabilizes, the  $\text{Ca}^{2+}$  bound N-terminal domain of TnC. Phosphorylation interferes with this interaction between TnI and TnC resulting in weaker  $\text{Ca}^{2+}$  binding. In this study, we used  $^1\text{H}$ - $^{15}\text{N}$ -HSQC NMR to investigate at the atomic level the interaction between an N-terminal fragment of TnI consisting of residues 1–64 of TnI (I1–64) and TnC. We produced several mutants of I1–64, TnI, and TnC to test the contribution of certain residues to the transmission of the phosphorylation signal in both NMR experiments and functional assays. We also investigated how phosphorylation of the PKC sites in I1–64 (S41 and S43) affects the interaction of I1–64 with TnC. We found that phosphorylation of S22 and S23 produced only localized effects in the structure of I1–64 between residues 24 and 34. Residues 1–17 of I1–64 did not bind to TnC, and residues 38–64 bound tightly to the C-terminal domain of TnC regardless of phosphorylation. Residues 22–34 bound weakly to TnC in a phosphorylation sensitive manner. Bisphosphorylation prevented this phosphorylation switch region from interacting with TnC. Systematic mutation of residues in the phosphorylation switch did not prevent PKA phosphorylation from accelerating  $\text{Ca}^{2+}$  release from troponin. We conclude that the phosphorylation switch binds to TnC via an extended interaction site spanning residues R19 to A34.

The troponin complex regulates the contractile activity of striated muscle in response to changes in the intracellular  $\text{Ca}^{2+}$  concentration. Troponin consists of three subunits: a  $\text{Ca}^{2+}$  binding subunit, troponin C (TnC);<sup>1</sup> an inhibitory subunit, troponin I (TnI); and a tropomyosin binding subunit, troponin T (TnT). The recent publication of the crystal structure of the core domain of human cardiac troponin (I) confirms much of the accumulated biochemical data as to how the three troponin subunits interact with one another. However, several important regions of the complex, such as the cardiac isoform specific N-terminal 30 residue extension of TnI and the inhibitory region of TnI, are absent or not resolved in the core domain structure.

TnT anchors the troponin complex to the thin (actin) filament and interacts with tropomyosin, TnI, and TnC (reviewed in ref 2). TnC is a calmodulin-like protein containing four EF-hand motifs organized into two domains (3). The two EF hands in the C-terminal domain bind  $\text{Ca}^{2+}$  (sites III and IV) with very high affinity (or  $\text{Mg}^{2+}$  with lower

affinity) and are believed to be involved in structural interactions with TnI and TnT. In cardiac TnC, site I in the N-terminal domain does not bind divalent cations, and site II, which binds  $\text{Ca}^{2+}$  with a moderate affinity, acts as the regulatory site whose  $\text{Ca}^{2+}$  occupancy controls muscle contraction. TnI binds to actin and TnC via several interaction sites (reviewed in ref 4). The C-terminal half of TnI is directly involved in the protein–protein interactions that regulate muscle. In the absence of  $\text{Ca}^{2+}$ , the inhibitory region of TnI (residues ~125–145 of cardiac TnI) binds to actin inhibiting muscle contraction (5, 6). In the presence of  $\text{Ca}^{2+}$ , the regulatory region of TnI (residues ~147–163 of cardiac TnI) binds to the N-terminal domain of TnC, and the inhibitory region is released from actin relieving inhibition (7). The N-terminal region of TnI (residues ~42–64) forms a helix that binds tightly to the C-terminal domain of TnC anchoring the two proteins together (1, 8, 9). C-terminal to this helix, TnI interacts with the T2 region of TnT via a coiled–coil (1, 10) and N-terminal to the helix is a 30-residue extension that is specific to the cardiac isoform of TnI.

In the heart, phosphorylation of TnI by protein kinases A and C provides a mechanism to fine-tune the regulatory properties of the troponin complex. PKA mediated phosphorylation of TnI was first demonstrated in 1976 (11, 12). The sites of phosphorylation have subsequently been shown to be S22 and S23 within the 30 residue N-terminal extension (13, 14). The effect of bisphosphorylation of the N-terminal extension of TnI is an acceleration of  $\text{Ca}^{2+}$  release from the regulatory  $\text{Ca}^{2+}$  site in the N-terminal domain of TnC. This

<sup>†</sup> This work was funded by the British Heart Foundation.

\* To whom correspondence should be addressed. Telephone: 44 (0)121 414 5401. Fax: 44 (0)121 414 5925. E-mail: i.p.trayer@bham.ac.uk.

<sup>1</sup> Abbreviations: TnC, troponin C; TnI, troponin I; TnT, troponin T; –12 TnC, troponin C with 12 residues deleted from the N-terminus; T2, residues 168–288 of TnT; I1–64, residues 1–64 of human cardiac TnI; N-terminal domain of TnC, residues 1–91 of TnC; C-terminal domain of TnC, residues 89–161 of TnC; PKA, protein kinase A; PKC, protein kinase C; U, unit of kinase activity equal to 1 nmol of phosphate transfer per minute; IAANS, 2-(4'-(iodoacetamido)anilino)naphthalene-6-sulfonic acid; HSQC, heteronuclear single quantum coherence.

results in a desensitization to  $\text{Ca}^{2+}$  in actomyosin ATPase or force measurements and faster relaxation in skinned myofibrils (11, 15–18). PKA mediated phosphorylation of TnI has also been shown to accelerate crossbridge kinetics (19, 20). PKC mediated phosphorylation of TnI results in phosphorylation of S22, S23, S41, S43, S76, and T142 in vitro (21), and transgenic approaches have demonstrated functional consequences of S41/S43 phosphorylation in vivo (22, 23). PKC mediated phosphorylation of TnI at S41 and S43 results in a decrease in maximal ATPase activity and force production and desensitization to  $\text{Ca}^{2+}$  (24–26).

The mechanisms that transmit the effects of TnI phosphorylation to the rest of the troponin complex are not fully understood. Fluorescence anisotropy studies (27) and neutron scattering data (28) show TnI undergoing significant shape changes upon PKA bisphosphorylation. The shape change may be due to a folding of the N-terminal extension following phosphorylation (29). This folding may be due to release of the N-terminal extension from an interaction with TnC as NMR, and cross-linking work, indicate that the unphosphorylated N-terminal extension of TnI binds to TnC and that bisphosphorylation prevents this binding from occurring (9, 30–32). The phosphorylation signal can be transmitted from TnI to TnC in minimal binary complexes such as TnI plus the N-terminal domain of TnC (33) or TnI truncated at residue 64 (I1–64) plus TnC (9). To date, the data suggest that large-scale conformational changes in the troponin complex do not underlie transmission of the phosphorylation signal from TnI to TnC. A localized mechanism involving phosphorylation sensitive binding of the N-terminal extension of TnI to the N-terminal domain of TnC seems to underlie the transmission process.

We have recently used one-dimensional (1-D)  $^1\text{H}$  NMR to study I1–64 in complex with TnC and demonstrated that residues close to S22 and S23 in the N-terminal extension (Y25 and Y28) are involved in phosphorylation sensitive binding to TnC (34). Because of the limited resolving power of 1-D NMR, we were unable to determine all of the TnI residues involved in this TnC interaction site that we refer to as the phosphorylation switch.

In this study, we produced a mutant TnC, –12 TnC, with the N-helix removed to test whether this region of TnC might provide the docking site for the phosphorylation switch region of TnI. We then returned to wt TnC and looked at how the phosphorylation of S41 and S43 by PKC modulates the interactions between I1–64 and TnC and whether there were additive effects of phosphorylating S22, S23 and S41, S43. We then used  $^1\text{H}$ - $^{15}\text{N}$ -HSQC NMR of  $^{15}\text{N}$  labeled I1–64, free and in complex with TnC, to extend our 1-D  $^1\text{H}$  NMR studies that demonstrated that the phosphorylation switch binds to TnC (34). Isotopic labeling of the I1–64 but not the TnC allowed us to investigate which residues of TnI bind to TnC (as supposed to previous studies that have focused on the TnC side of the interaction (30–32)). We were able to assign the HSQC peaks of many of the backbone amide groups of I1–64, and this allowed us to determine exactly which residues of TnI form the phosphorylation switch. We completed the study by site-directed mutagenesis of phosphorylation switch residues in full-length TnI and measurement of the effects of these mutations on  $\text{Ca}^{2+}$  release from the troponin complex.

## EXPERIMENTAL PROCEDURES

**Protein Preparation.** Recombinant human cardiac TnT, TnI, and TnC and mutants thereof were expressed in *Escherichia coli* and purified as described previously (35). Mutations were introduced using the mega-primer PCR method. I1–64 was produced by CNBr digestion of a mutant TnI with a methionine residue introduced at position 64 and the naturally occurring methionines converted to leucine. The I1–64 was purified from the CNBr digest of the mutant TnI by reverse-phase HPLC (Vydac C5 semi-prep column) in 0.1% trifluoroacetic acid with a 25–45% acetonitrile gradient (9). Purity and identity were checked by SDS–PAGE and MALDI-TOF mass spectrometry.  $^{15}\text{N}$  labeled TnI fragments were prepared from TnI expressed using minimal medium supplemented with  $^{15}\text{NH}_4\text{Cl}$  (GOSS Scientific Instruments). Protein concentrations were determined using the bicinchoninic acid protein assay (Pierce) calibrated with bovine serum albumin.

**PKA Phosphorylation of I1–64.** I1–64 was dissolved at 5 mg/mL in 300 mM KCl, 20 mM MOPS/KOH (pH 7.0), 3 mM  $\text{MgCl}_2$ , and 2.5 mM  $\text{ATPN}_2$ , 1 mM DTT. Porcine PKA catalytic subunit (Sigma) was added to a final concentration of 0.25 U/mL, and the phosphorylation was allowed to proceed overnight at room temperature. The phosphorylated I1–64 was purified by HPLC (as stated previously), and the extent of phosphorylation was determined by MALDI-TOF mass spectrometry.

**PKC Phosphorylation of I1–64.** I1–64 was dissolved at 0.7 mg/mL in 150 mM KCl, 20 mM MOPS/KOH (pH 7.0), 10 mM  $\text{MgCl}_2$ , 2.5 mM  $\text{ATPN}_2$ , 1 mM DTT, 0.5 mM  $\text{CaCl}_2$ , 20  $\mu\text{g/mL}$  phosphatidylserine, and 5  $\mu\text{g/mL}$  diolein. Human recombinant PKC $\alpha$  (Calbiochem) was added to a final concentration of 4 U/mL, and the phosphorylation was allowed to proceed overnight at 30 °C (or 40 U/mL PKC $\alpha$  and varying times in the experiment of Figure 2). The phosphorylated I1–64 was purified by HPLC prior to use.

**MALDI-TOF Mass Spectrometry.** I1–64 mass spectra were collected using a Bruker Biflex IV spectrometer with  $\alpha$ -cyano-4-hydroxy-cinnamic acid as the matrix. Samples were desalted either by reverse-phase HPLC or using Zip Tips (Millipore). 100 shots were collected for each sample, and the quantity of each +80 mass unit phosphospecies was calculated from the peak heights (each phosphorylated species produced a separate distinct peak).

**NMR Spectroscopy.** All spectra were collected on a Bruker 500 MHz NMR spectrometer equipped with a cryoprobe. 1-D spectra were collected using a 5 kHz (10 ppm) spectral width with a relaxation delay of 3 s to enable complete magnetization recovery. Two-pulse spin–echo spectra were obtained using a 90- $\tau$ -180- $\tau$  sequence (36) with a delay time,  $\tau = 60$  ms ( $\tau = 1/2J$  and coupling constant,  $J$ , of 8.5 Hz (37). The delay after the nonselective 180 pulse allows the shifts but not  $J$ -modulations to be refocused such that dephasing due to magnetic field inhomogeneity is reversed at  $2\tau$  and the magnetization can be said to form a spin–echo. Typically 128 scans were acquired at 293 K using 150  $\mu\text{M}$  protein dissolved in 20 mM KCl, 20 mM  $d_{11}$ -Tris, 2.5 mM  $\text{CaCl}_2$  in  $\text{D}_2\text{O}$  at pH 7.4. Samples were prepared by dissolving the protein in buffer, adjusting the pH (when necessary), and spinning at 45 000 rpm for 20 min (Beckman TL-100) to remove any insoluble material. Two-dimensional

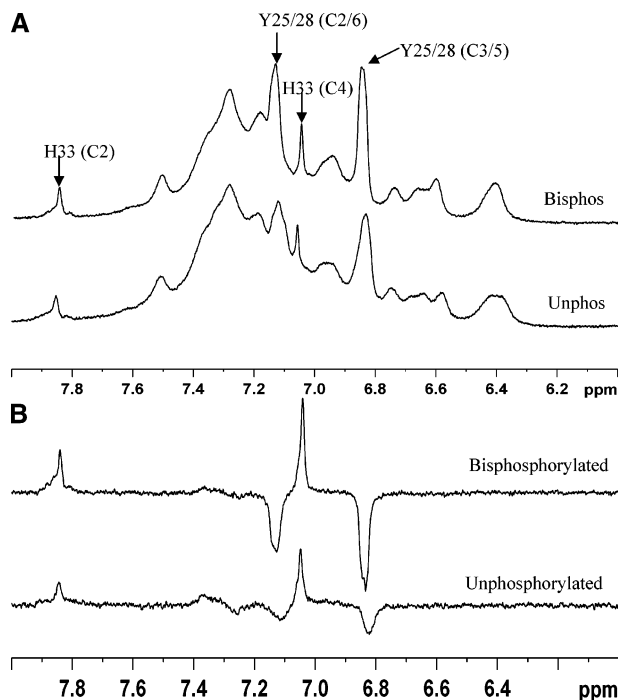


FIGURE 1: 1-D  $^1\text{H}$  NMR spectra of unphosphorylated and bisphosphorylated I1-64. -12 TnC complex. Spectra were obtained at 20  $^\circ\text{C}$  as described in Experimental Procedures. Panel A shows the aromatic region of the 1-D  $^1\text{H}$  NMR spectra of 150  $\mu\text{M}$  unphosphorylated or bisphosphorylated I1-64 plus 150  $\mu\text{M}$  -12 TnC. Panel B shows two-pulse spin-echo spectra of the same samples.

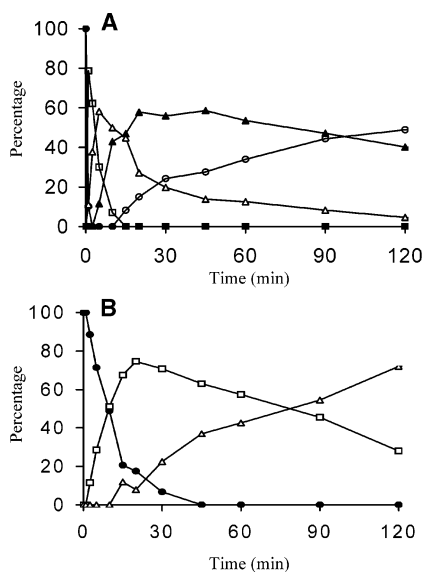


FIGURE 2: Time-course of PKC $\alpha$  phosphorylation of I1-64 (A) and S22/23A I1-64 (B). Phosphorylation was carried out as described in Experimental Procedures. At the times indicated, aliquots were taken and mixed with 3 volumes of chilled 0.1% trifluoroacetic acid prior to desalting with Zip Tips. The phosphorylation status of the I1-64 was then assessed by mass spectrometry. Symbols used are unfilled circles; unfilled squares; unfilled triangles; filled circles; and filled triangles.

spectra were collected using standard protocols. Gradient sensitivity-enhanced HSQC spectra were acquired at 285 K with 1024 and 128 complex points in the  $^1\text{H}$  ( $t_2$ ) and  $^{15}\text{N}$  ( $t_1$ ) dimensions, respectively, and spectral widths of 5500 ( $^1\text{H}$ ) and 1520 Hz ( $^{15}\text{N}$ ) using 200  $\mu\text{M}$   $^{15}\text{N}$ -labeled I1-64  $\pm$

250  $\mu\text{M}$  TnC in 200 mM KCl, 20 mM MES, 2.5 mM  $\text{CaCl}_2$ , 1 mM DTT in  $\text{H}_2\text{O}$  at pH 6.3. External DSS was used to provide the  $^1\text{H}$  chemical shift reference standard (0.00 ppm), and  $^{15}\text{N}$  chemical shifts were referenced indirectly assuming an absolute frequency ratio ( $^{15}\text{N}/^1\text{H}$ ) = 0.10132912. Resonance assignments for I1-64 were derived from a combination of HSQC-TOCSY (mixing period = 60 ms) and HSQC-NOESY (mixing period 300–600 ms) spectra that were acquired using samples containing 3 mM I1-64 in  $\text{H}_2\text{O}$  at pH 5.3. The combined  $^1\text{H}$ - $^{15}\text{N}$  chemical shift differences plotted in Figures 4B and 7B were calculated as the square root of the sum of the  $^1\text{H}$  shift change squared plus one tenth of the  $^{15}\text{N}$  shift change squared (the weighting makes the  $^1\text{H}$  and  $^{15}\text{N}$  contributions approximately equal) (38).

**Isothermal Titration Microcalorimetry.** All experiments were carried out using a Microcal Inc isothermal titration microcalorimeter. Experimental conditions were 300 mM KCl, 20 mM MOPS/KOH (pH 7.0), 3 mM  $\text{MgCl}_2$ , 0.5 mM EGTA  $\pm$  1 mM  $\text{CaCl}_2$  and 30  $^\circ\text{C}$ . The 1.4 mL sample cell was filled with 6  $\mu\text{M}$  ( $-\text{Ca}^{2+}$ ) I1-64 or 3  $\mu\text{M}$  I1-64 ( $+\text{Ca}^{2+}$ ) and titrated with 5  $\mu\text{L}$  injections of 160  $\mu\text{M}$  TnC ( $-\text{Ca}^{2+}$ ) or 60  $\mu\text{M}$  TnC ( $+\text{Ca}^{2+}$ ). Binding parameters were obtained using the Origin-ITC data analysis software package in single set of sites mode.

**$\text{Ca}^{2+}$  Off-Rate Measurements.** A C84S mutant of human cardiac TnC was labeled at Cys-35 with IAANS (18). The IAANS-labeled TnC was then reconstituted into troponin by mixing with TnI and TnT in a 1:1:1 molar ratio in 8 M urea, 25 mM triethanolamine (pH 7.5), 1 mM dithiothreitol, and 1 mM  $\text{CaCl}_2$ . The troponin was dialyzed extensively against stopped-flow buffer (100 mM KCl, 20 mM MOPS/KOH (pH 7.0), 3 mM  $\text{MgCl}_2$ , 50  $\mu\text{M}$   $\text{CaCl}_2$ ) at 4  $^\circ\text{C}$ . The troponin was then diluted to 5  $\mu\text{M}$ , and 1 mM ATP was added and incubated at 25  $^\circ\text{C}$  for 1 h with or without 50 units PKA/mL (the PKA was previously dialyzed against stopped-flow buffer). The troponin was diluted to 1  $\mu\text{M}$  in stopped-flow buffer prior to use. The rate of  $\text{Ca}^{2+}$  release from the troponin was determined from the increase in IAANS fluorescence when 90  $\mu\text{L}$  of the  $\text{Ca}^{2+}$  saturated troponin was rapidly mixed with 10  $\mu\text{L}$  of 100 mM EGTA/KOH (pH 7.0) at 25  $^\circ\text{C}$  (Applied Photophysics SX-18MV stopped-flow fluorimeter) ( $\lambda_{\text{excitation}}$  = 325 nm, 400 nm filter). Rate constants were calculated by least-squares fitting of the data to a single-exponential function.

## RESULTS

### $^1\text{H}$ NMR Analysis of I1-64 in Complex with -12 TnC.

Figure 1A shows the aromatic region of the 1-D  $^1\text{H}$  NMR spectra of unphosphorylated and PKA bisphosphorylated I1-64 in complex with -12 TnC. This mutant TnC with 12 residues deleted from the N-terminus was designed to test the importance of the N-helix of TnC to the interaction between the phosphorylation switch and TnC. We have previously shown that the NMR peaks from the side chains of Y25, Y28, and H33 of I1-64 act as particularly good reporters of the binding of the phosphorylation switch region of I1-64 to wt TnC (34). -12 TnC induced broadening of the peaks from these residues is evident in the lower spectrum of Figure 1A. In the spectrum of the bisphosphorylated complex (upper spectrum in Figure 1A) the Y25, Y28, and H33 peaks are considerably sharper than in the unphos-

phorylated complex (lower spectrum in Figure 1A). This shows that, as with wt TnC, the phosphorylation switch of unphosphorylated I1–64 binds to –12 TnC, and phosphorylation prevents this binding. It would appear that the N-helix of TnC does not form the primary binding site for the phosphorylation switch. Figure 1B shows the aromatic region of the two-pulse spin-echo spectra of the unphosphorylated and bisphosphorylated I1–64–12 TnC complexes. Spectral accumulation in this way distinguishes resonances on the basis of their  $J$ -coupling patterns (36). Since signal amplitude in these experiments is modulated by the corresponding coupling constant and  $T_2$  relaxation time of each resonance, the amplitudes of the peaks in these spectra are very sensitive to the effects of binding. The sharp doublet side-chain resonances of Y25 and Y28 of I1–64 appear inverted, while the phase of the singlet resonances of H33 of I1–64 is unaltered in these  $J$ -modulated spectra. These spectra provide particularly clear evidence that bisphosphorylation weakens the interaction between the phosphorylation switch and –12 TnC.

The broadening of the Y25, Y28, and H33 signals by –12 TnC is somewhat greater than that previously reported with wt TnC (34). This may arise from a change in the dynamics of the N-terminal domain of TnC or the dynamics of the interaction between the phosphorylation switch and the N-terminal domain of TnC. What is clear is that, if introducing a mutation in the N-terminal domain of TnC alters the influence that TnC has over the phosphorylation switch, there must be a linkage between these regions of TnC and TnI. To check that the –12 mutation was not grossly influencing the properties of TnC, we used 1-D  $^1\text{H}$  NMR to follow  $\text{Ca}^{2+}$  titrations of wt and –12 TnC (data not shown). The  $\text{Ca}^{2+}$  binding properties of the two proteins were not detectably different indicating that –12 TnC retains the ability to bind  $\text{Ca}^{2+}$  at the regulatory site and would be fully saturated in the experiments of Figure 1A,B.

**PKC Phosphorylation of I1–64.** We used MALDI-TOF mass spectrometry to follow the time-course of PKC $\alpha$  mediated phosphorylation of I1–64 (Figure 2A). We found that PKC $\alpha$  phosphorylates I1–64 to a maximal tetra-kis phosphospecies. Two sites appear to be phosphorylated rapidly, whereas incorporation of the third and fourth phosphates is much slower. HSQC analysis of tetra-kis phosphorylated  $^{15}\text{N}$  labeled I1–64 demonstrated that S22, S23, S41, and S43 were the phosphorylated residues (data not shown). To produce I1–64 phosphorylated exclusively at S41 and S43, we produced a S22/23A mutant of I1–64 to prevent phosphorylation at S22 and S23. The time-course of PKC $\alpha$  mediated phosphorylation of S22/23A I1–64 is shown in Figure 2B. In this case, the maximal extent of phosphorylation is bisphosphorylation. Monophosphorylation of S22/23A I1–64 is fairly rapid, although much slower than in wt I1–64. The bisphosphorylation of S22/23A I1–64 is much slower than the monophosphorylation suggesting that the first phosphorylation event impedes the second (as seen with PKA phosphorylation of S22 and S23 (39)). Under these conditions, the favored phosphorylation sites for PKC $\alpha$  on I1–64 appear to be S22 and S23 as the rates of mono and bisphosphorylation of S22/23A I1–64 are very similar to the rates of tri- and tetra-kisphosphorylation of I1–64.

**Binding of PKC Phosphorylated I1–64 to wt TnC.** We used isothermal titration microcalorimetry to measure the

Table 1: Binding Stoichiometry ( $n$ ), Affinity ( $K$ ), and Enthalpy ( $\Delta H$ ) of Complex Formation between PKC Bisphosphorylated S22/23A I1–64 and PKC Tetra-kisphosphorylated I1–64 and TnC<sup>a</sup>

	$n$	$K_a \cdot 10^{-7} (\text{M}^{-1})$	$\Delta H (\text{kcal/mol})$
S22/23A bis ( $-\text{Ca}^{2+}$ )	$0.75 \pm 0.04$	$0.77 \pm 0.13$	$-7.7 \pm 0.3$
S22/23A bis ( $+\text{Ca}^{2+}$ )	$0.63 \pm 0.01$	$7.8 \pm 1.1$	$-17.0 \pm 0.8$
tetra-kis ( $-\text{Ca}^{2+}$ )	$0.96 \pm 0.07$	$0.45 \pm 0.06$	$-6.94 \pm 0.32$
tetra-kis ( $+\text{Ca}^{2+}$ )	$0.85 \pm 0.06$	$8.3 \pm 0.4$	$-14.7 \pm 0.8$

<sup>a</sup> Data represent the mean ( $\pm$ SEM) of six isothermal microcalorimetric titrations. Phosphorylation and microcalorimetry were carried out as described in Experimental Procedures.

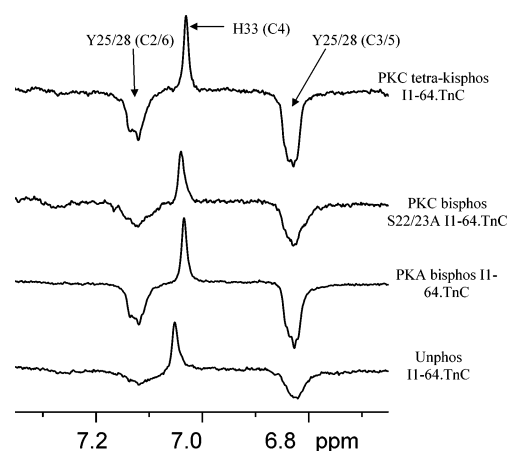


FIGURE 3: Two-pulse spin-echo spectra of PKA and PKC phosphorylated I1–64·TnC complexes. Samples were prepared at 150  $\mu\text{M}$  I1–64 plus 150  $\mu\text{M}$  TnC, and spectra were collected as described in Experimental Procedures. Although only the aromatic region is shown (for clarity), the alanine region of the spectra was used to normalize the vertical scaling.

binding of bisphosphorylated S22/23A I1–64 (phosphorylated at S41 and S43) and tetra-kis phosphorylated I1–64 (phosphorylated at S22, S23, S41, and S43) to TnC (Table 1). The binding constants can be compared with  $2.97 \pm 0.37 \times 10^7 \text{ M}^{-1}$  in the absence of  $\text{Ca}^{2+}$  and  $10.9 \pm 4.5 \times 10^7 \text{ M}^{-1}$  in the presence of  $\text{Ca}^{2+}$  for unphosphorylated I1–64 binding to TnC (9). PKC mediated bisphosphorylation at S41 and S43 produces a 4-fold decrease in the affinity of I1–64 for TnC in the absence of  $\text{Ca}^{2+}$ . Tetra-kis phosphorylation of I1–64 produces a 6-fold decrease in affinity for TnC in the absence of  $\text{Ca}^{2+}$ : the small reduction in affinity between I1–64 and TnC upon S22/23 bisphosphorylation that we have previously reported (9) and the effect of S41/43 bisphosphorylation on the affinity appear to be additive. In the presence of  $\text{Ca}^{2+}$ , S41/43 bisphosphorylation has little effect on the tight binding of I1–64 to TnC ( $K_a \sim 1 \times 10^8 \text{ M}^{-1}$ ). Phosphorylation of S41 and S43 also does not substantially alter the binding enthalpy or stoichiometry of I1–64 binding to TnC.

**$^1\text{H}$  NMR Analysis of PKC Phosphorylated I1–64 in Complex with TnC.** Figure 3 shows the aromatic region of the two-pulse spin-echo spectra of I1–64·TnC complexes in various states of phosphorylation. The spectrum of the unphosphorylated complex shows the 2/6 and 3/5 peaks of Y25 and Y28 substantially broadened. In the PKA bisphosphorylated complex, the tyrosine peaks are much sharper and have undergone small shifts toward their positions in the free peptide indicating that phosphorylation of S22/23 weakens the interaction between the phosphorylation switch and TnC. In the PKC bisphosphorylated S22/23A I1–64·

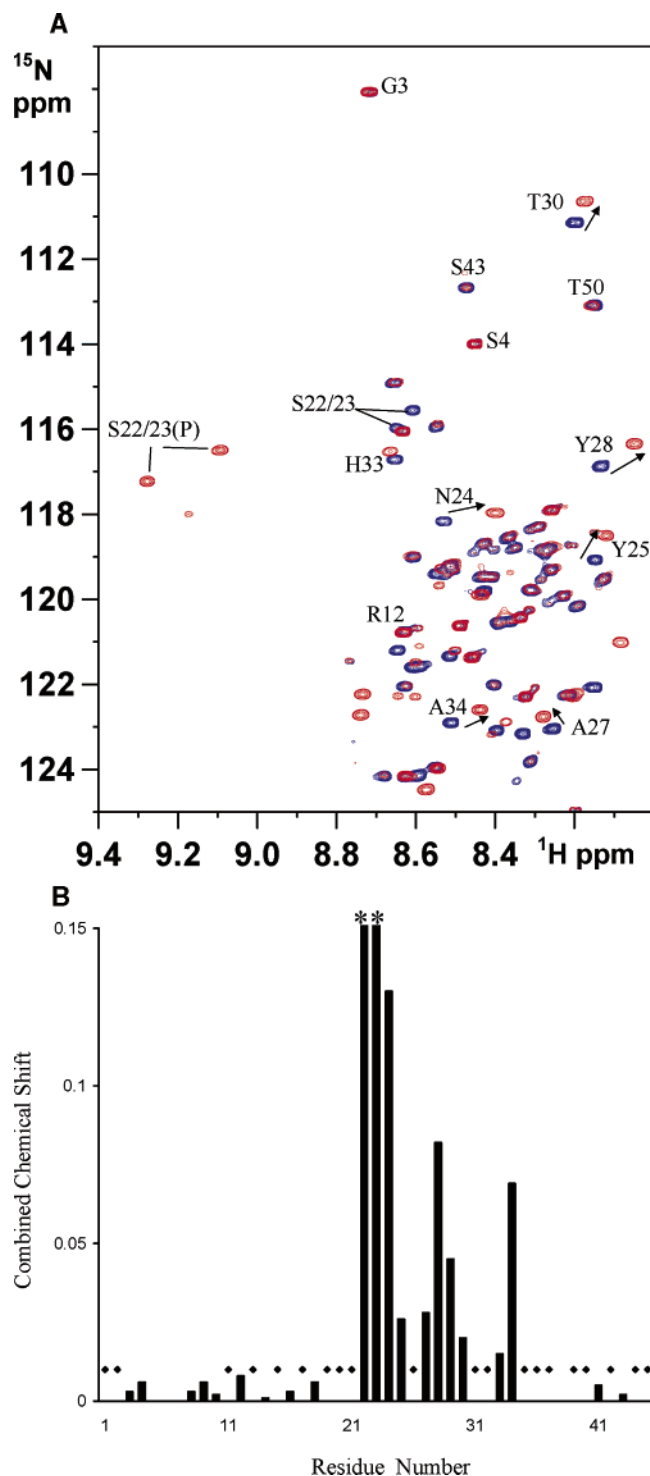


FIGURE 4: HSQC of unphosphorylated and bisphosphorylated  $^{15}\text{N}$  labeled I1–64. Panel A shows the HSQC spectra of unphosphorylated I1–64 (blue) and bisphosphorylated I1–64 (red). Several of the bisphosphorylation induced shifts are indicated with arrows. Panel B plots the bisphosphorylation induced change in the combined weighted  $^1\text{H}$ - $^{15}\text{N}$  chemical shift (calculated as described in Experimental Procedures) against residue number. Diamond symbols indicate unassigned (or proline) residues. The phosphorylation induced shifts of S22 and S23 (marked with asterisks) are off the scale of this plot ( $\sim 0.5$ ).

TnC complex, the signals from Y25 and Y28 are very similar to those in the unphosphorylated complex. This demonstrates that phosphorylation of S41 and S43 of I1–64 does not alter the interaction between the phosphorylation switch and TnC. The tyrosine peaks in the spectrum of the tetra-kisphos-

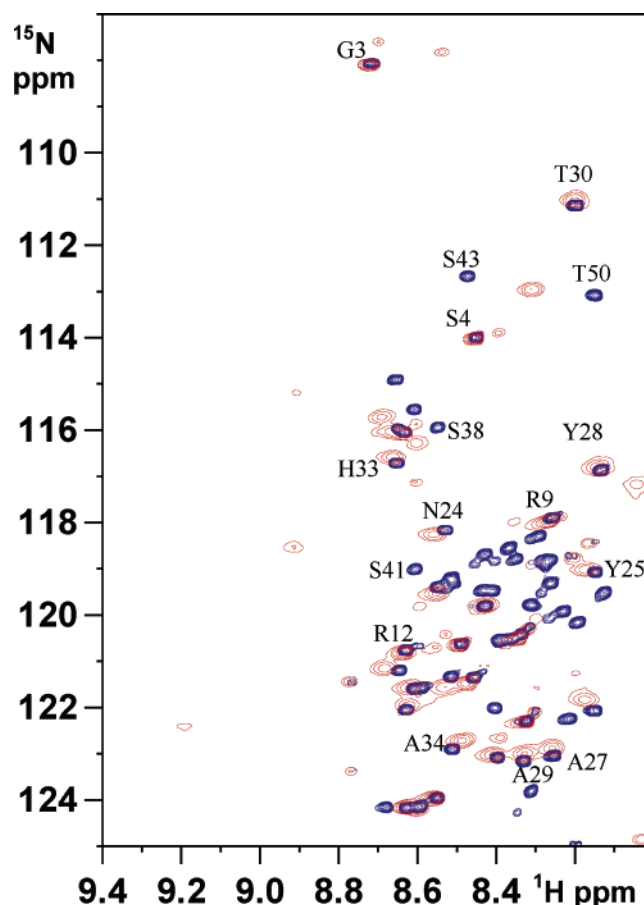


FIGURE 5: HSQC spectra of  $^{15}\text{N}$  labeled I1–64, free and in complex with TnC. Free I1–64 peaks are shown in blue, and complexed I1–64 peaks are in red. Representative peaks from the N-terminal region, the phosphorylation switch, and the C-terminal region of I1–64 have been labeled.

phorylated complex are very similar to those of PKA bisphosphorylated complex (i.e., phosphorylation at S41 and S43 does not interfere with S22/23 bisphosphorylation weakening the binding of the phosphorylation switch to TnC). We conclude that the structural changes underlying the effects of S22/23 and S41/43 bisphosphorylation are distinct and independent.

**HSQC Analysis of  $^{15}\text{N}$  Labeled I1–64.** Figure 4A shows the HSQC spectra of unphosphorylated and PKA bisphosphorylated I1–64. Signals arising from the backbone amide groups of residues N24 to A34 are shifted by bisphosphorylation (Figure 4A,B). HSQC spectra provide a sensitive indicator of peptide backbone conformational changes, and the signals arising from the remainder of I1–64 are not affected by phosphorylation. Therefore, while bisphosphorylation may induce localized conformational changes, these structural changes are not conducted throughout I1–64.

**HSQC Analysis of I1–64•TnC Complexes.** The differences in the backbone amide signals between free I1–64 and I1–64 in complex with TnC (Figure 5) indicate a change of environment induced by proximity to TnC. TnC has very different effects on three distinct regions of I1–64. Binding of TnC to I1–64 induces shifts or disappearances of signals from the C-terminal region of I1–64 (residues 38–64). This is consistent with this region of TnI forming an  $\alpha$ -helix that binds tightly in the hydrophobic cleft of the C-terminal

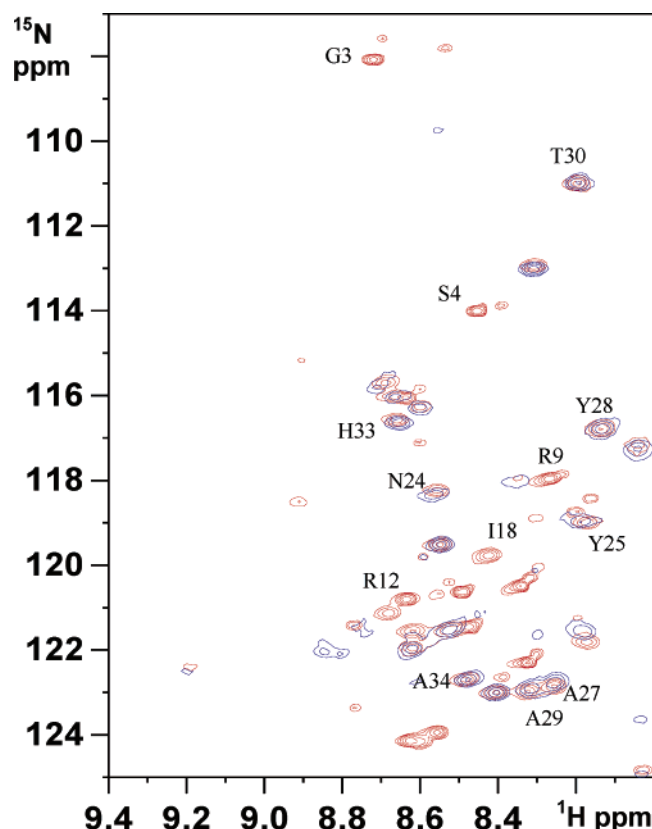


FIGURE 6: Comparison of the HSQC spectra of  $^{15}\text{N}$  labeled I1–64 in complex with TnC (red) and  $^{15}\text{N}$  labeled I19–64 in complex with TnC (blue). Several resonances from backbone amide groups common to I1–64 and I19–64 and peaks present only in I1–64 (but deleted in I19–64) have been labeled.

domain of TnC (1, 8). The disappearance (line-broadening) of signals arises from intermediate exchange. The very high affinity of I1–64 for TnC (9) (and hence slow dissociation rate of the complex) dictates that the line-broadening does not arise from exchange between free and bound I1–64 but between different bound conformations of residues 38–64 of I1–64 while bound in the hydrophobic cleft of the C-terminal domain of TnC. A second region of I1–64, residues 1–18, is not strongly influenced by TnC although the amide group signals of E10 and R12 do shift slightly in response to the addition of TnC suggesting that a weak interaction between these residues and TnC could occur. Signals from residues N-terminal to E10 are not affected by TnC, demonstrating that the extreme N-terminal region of TnI does not bind to TnC. Signals arising from residues 22–38 undergo small shifts or broadening in the presence of TnC showing that this region of unphosphorylated I1–64 binds to TnC (see also Figure 7B).

HSQC spectra were collected using mutants of TnC and  $^{15}\text{N}$ -labeled I1–64 to further characterize the interactions between the two proteins. HSQC experiments with two N-terminal deletion mutants of I1–64 (I10–64 and I19–64), both free and in complex with TnC, gave identical spectra to I1–64 (except for the absence of signals from the deleted residues). Figure 6 compares the HSQC spectra of I1–64·TnC and I19–64·TnC. Removing the N-terminal 18 residues of I1–64 does not shift the resonances arising from residues 22–38, demonstrating that the N-terminal region of I1–64 does not influence the conformation, or TnC binding properties, of I1–64 C-terminal to the phosphoryl-

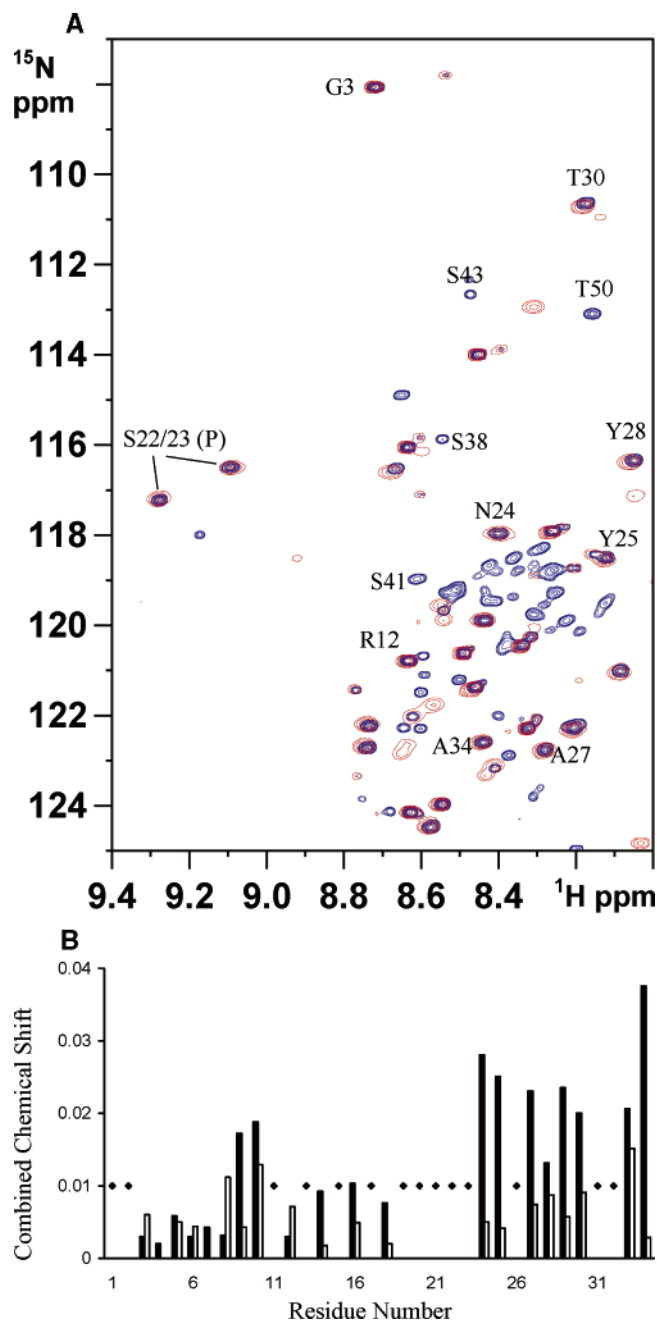


FIGURE 7: HSQC of bisphosphorylated I1–64, free and in complex with TnC. Panel A shows the HSQC spectra of free PKA bisphosphorylated I1–64 (blue) and TnC bound bisphosphorylated I1–64 (red). Panel B plots the weighted combined shift changes induced by TnC binding to unphosphorylated (solid black bars) and bisphosphorylated (hollow bars) I1–64. Diamond symbols indicate unassigned (or proline) residues. The combined shifts were calculated as described in Experimental Procedures.

ation sites. Binding of the TnC mutant, E76A TnC (which is unable to bind  $\text{Ca}^{2+}$  at the regulatory site (34)), produced very similar shifts in the HSQC spectrum of  $^{15}\text{N}$ -labeled I1–64 of to the binding of wt TnC (data not shown). This demonstrates that, although  $\text{Ca}^{2+}$  may influence the binding of the phosphorylation switch to TnC (34), this binding can still occur when the regulatory site does not have  $\text{Ca}^{2+}$  bound. We also tested for interactions with TnT by adding an equimolar quantity of T2 (residues 168–288 of TnT) to the I1–64·TnC complex. T2 did not produce any shifts indicating a lack of interaction between I1–64 and the T2 region

of TnT under these conditions, although the T2 would be expected to bind to the TnC ( $K_a$  for T2 binding to TnC  $\sim 4 \times 10^6 \text{ M}^{-1}$ , Fairhead and Trayer, unpublished data).

**HSQC Analysis of Bisphosphorylated I1–64•TnC Complexes.** Figure 7A shows the overlaid HSQC spectra of bisphosphorylated I1–64 and bisphosphorylated I1–64 in complex with TnC. Binding of TnC to bisphosphorylated I1–64 does not affect the backbone amide groups of phosphoserines 22 and 23. The phosphoserine residues are, therefore, not directly involved in binding to TnC. Figure 7B allows comparison of the effects of TnC on unphosphorylated and bisphosphorylated I1–64. Signals from residues C-terminal to phosphoserines 22 and 23 (N24 to A34) are shifted by TnC to a far lesser extent than in the unphosphorylated complex. This implies that the binding of the phosphorylation switch region of I1–64 to TnC is substantially weakened by bisphosphorylation. As in the unphosphorylated complex, residues 1–18 of bisphosphorylated I1–64 are not strongly influenced by TnC. Bisphosphorylation does not interfere with the binding of residues 38–64 of I1–64 to TnC.

When we replaced bisphosphorylated I1–64 with bisphosphorylated I10–64, we found that deleting residues 1–9 had no effect on the remainder of the spectrum. However, in the bisphosphorylated I19–64•TnC complex, the backbone amide groups of phosphoserines 22 and 23, N24, and Y25 gave multiple signals indicative of multiple conformations (data not shown). It may be that some, or all, of the residues between 10 and 18 of I1–64 are required to maintain the bisphosphorylation induced conformational changes in the phosphorylation switch. The spectra of the bisphosphorylated I1–64•E76A TnC and I1–64•TnC•T2 complexes were essentially the same as that of bisphosphorylated I1–64•TnC indicating that, like the unphosphorylated state, the bisphosphorylated N-terminal extension does not bind to T2 and is not influenced by the  $\text{Ca}^{2+}$  occupancy of the regulatory site.

**HSQC Analysis of Monophosphorylated  $^{15}\text{N}$  Labeled I1–64.** We used S22A and S23A mutants of I1–64 to produce the S23(P) and S22(P) monophosphorylated species, respectively. We then examined the effect of each monophosphorylation on the phosphorylation switch and its ability to interact with TnC. Both monophosphorylations produce localized chemical shifts in I1–64. However, neither monophosphorylation prevented binding of residues 24–34 to TnC as observed with bisphosphorylation.

**Effects of TnI Mutations on the Rate of  $\text{Ca}^{2+}$  Release from Troponin.** The fluorescence emission of IAANS attached to Cys-35 of TnC is reduced by approximately 25% when  $\text{Ca}^{2+}$  binds to site II in the troponin complex. We have used the corresponding fluorescence increase when  $\text{Ca}^{2+}$  is rapidly chelated in stopped-flow experiments to investigate the effects of phosphorylation and mutation of TnI on the rate of  $\text{Ca}^{2+}$  release from troponin. We have used a series of mutant full-length TnIs to investigate the importance of TnI residues around the phosphorylation sites. Two of the mutants date from our earlier cross-linking study (9) (I18C and R26C), whereas the others were designed specifically for this study. Two of the mutants (S22A and S23A) allowed us to investigate how monophosphorylation of the N-terminal extension of TnI influences the  $\text{Ca}^{2+}$  binding properties of the troponin complex.

Table 2:  $\text{Ca}^{2+}$  Dissociation Rates from Troponin Containing Mutant TnI and IAANS Labeled C84S TnC<sup>a</sup>

TnI mutant	UN off rate	PHOS off rate	% increase
wt	24.0 $\pm$ 0.5	32.2 $\pm$ 0.5	34
I18C	23.6 $\pm$ 0.3	32.5 $\pm$ 0.6	38
P32A	25.4 $\pm$ 0.2	34.5 $\pm$ 0.5	36
R26C	28.6 $\pm$ 0.4	43.2 $\pm$ 0.7	51
NA24/27II	29.8 $\pm$ 0.5	37.4 $\pm$ 0.6	26
YY25/28AA	31.1 $\pm$ 0.4	41.7 $\pm$ 0.9	34
S22/23A	24.0 $\pm$ 0.4		
S22/23D		31.2 $\pm$ 0.4	30
AAASS	29.0 $\pm$ 0.5		
AAADD		42.3 $\pm$ 0.6	46
S22A	26.5 $\pm$ 0.2	29.6 $\pm$ 0.3	12
S23A	26.4 $\pm$ 0.2	29.9 $\pm$ 0.2	13

<sup>a</sup> Rate constants ( $\text{s}^{-1}$ ) were determined by stopped-flow fluorescence spectroscopy at 25 °C as described in Experimental Procedures. The data represent the mean of at least six measurements ( $\pm$ SEM). UN indicates unphosphorylated TnI, and PHOS represents either PKA bisphosphorylated or S22/23D pseudophosphorylated. Percent increase indicates the percentage increase in the rate of  $\text{Ca}^{2+}$  release produced by bisphosphorylation or by the comparison of S22/23D with S22/23A or AAADD (R19/20/21A, S22/23D) with AAASS (R19/20/21A).

We have previously reported that troponin containing wt TnI releases  $\text{Ca}^{2+}$  at 24  $\text{s}^{-1}$ , which increases to 32  $\text{s}^{-1}$  upon phosphorylation, or to 41  $\text{s}^{-1}$  if the influence of the N-terminal extension is completely removed by deleting residues 1–29 (18). We would therefore predict that any mutation capable of totally preventing the N-terminal extension of TnI from binding to TnC would produce a  $\text{Ca}^{2+}$  release rate of 41  $\text{s}^{-1}$ .

The rate constants obtained for  $\text{Ca}^{2+}$  release from troponin containing the various TnI mutants are listed in Table 2. We selected P32 as a residue to mutate because it might act as a helix terminator or form a hinge or turn immediately C-terminal to the N-terminal extension. However, the  $\text{Ca}^{2+}$  release rates obtained with both I18C and P32A are very similar to those obtained with wt TnI. The HSQC spectrum of the I1–64•TnC complex indicates that I18 is not strongly influenced by binding to TnC or phosphorylation and may delineate the N-terminal limit of the phosphorylation switch. Likewise, P32, although it is within the region of I1–64 that binds to TnC in a phosphorylation sensitive manner according to the HSQC spectra, does not seem to play an important role in orientating the phosphorylation switch relative to TnC.

One single mutant, R26C, and two double mutants, NA24/27II and YY25/28AA, show  $\text{Ca}^{2+}$  off-rates increased by 20–30%, consistent with TnI residues between 24 and 28 being involved in stabilizing  $\text{Ca}^{2+}$  bound TnC. These mutations change the side-chain characteristics of residues that our NMR experiments indicate bind to TnC in a phosphorylation sensitive manner. These residues are also involved in localized structural changes that occur upon phosphorylation of synthetic peptides (39), but we see no disruption of the phosphorylation effect: the effect of phosphorylation is preserved in these mutants. Indeed, the effect of the mutations and phosphorylation appear to be additive, combining to increase the  $\text{Ca}^{2+}$  off-rate to approximately 40  $\text{s}^{-1}$ .

We have created four mutants to test the importance of residues R19 to S23. In the S22/23A mutant, S22 and S23 were converted to alanine. The resulting TnI behaved exactly as unphosphorylated wt TnI. In S22/23D, S22 and S23 were converted to aspartic acid successfully mimicking bisphos-

phorylated TnI, as reported previously (15). We then used the S22/23D pseudophosphorylation to probe the importance of R19, R20, and R21. Mutation of these arginines to alanine in wt TnI (AAASS) produced a 20% increase in  $\text{Ca}^{2+}$  off-rate demonstrating that one, or more, of the arginines is important in the binding of the phosphorylation switch to TnC. If the triple arginine to alanine mutation is combined with the S22/23D pseudophosphorylation (AAADD), the  $\text{Ca}^{2+}$  off-rate increases to  $42 \text{ s}^{-1}$ . This experiment again shows additive effects of mutation and phosphorylation consistent with the mode of action of TnI phosphorylation being a weakening of the interaction between the N-terminal extension of TnI and TnC. Electrostatic interactions have previously been demonstrated between S22(P) and S23(P) and the preceding arginine residues in bisphosphorylated TnI (39, 40). The pseudophosphorylation effect that we observe in the absence of R19, R20, and R21 shows that these interactions are not the only mechanism underlying the effect of phosphorylation.

Treatment of troponin containing the S22A or S23A TnI mutant with PKA creates the monophosphorylated TnI species S23(P) and S22(P), respectively. We find that either monophosphorylation produces an increase in  $\text{Ca}^{2+}$  off rate of 12–13%. This increase is nearly half that produced by bisphosphorylation suggesting that sequential phosphorylation of serines 22 and 23 affects  $\text{Ca}^{2+}$  release in a stepwise manner (as has been reported for the affinity between troponin subunits (41)).

## DISCUSSION

The NMR spectra of the I1–64·TnC complexes that we have presented here demonstrate that residues around S22 and S23 of unphosphorylated TnI bind to the N-terminal domain of TnC in a phosphorylation sensitive manner. The N-terminal limit of this phosphorylation switch region of TnI lies between R19 and R21 as determined by the effect of mutating R19, R20, and R21 on the rate of  $\text{Ca}^{2+}$  release. The C-terminal limit of this region lies between A34 and S38 as determined from the HSQC of unphosphorylated and bisphosphorylated I1–64·TnC complex: the signals from A34 and S38 both shift in response to TnC binding to unphosphorylated I1–64, but with bisphosphorylated I1–64, S38 shifts whereas A34 does not. The phosphorylation switch binds to TnC when S22 and S23 are unphosphorylated or if one or other is phosphorylated. Bisphosphorylation of S22 and S23 prevents the phosphorylation switch from binding to TnC (although in our I1–64·TnC model system, the I1–64 will still be bound to the C-terminal domain of TnC). Bisphosphorylation of I1–64 (in the absence of TnC) alters the environments of the backbone amide groups of the phosphorylation switch, indicating that phosphorylation may induce localized conformational changes around S22 and S23, as previously reported in shorter peptides (39, 42). These conformational changes may underlie the disruption of TnC binding caused by bisphosphorylation. Mutation of residues within the phosphorylation switch did not reveal any residues that are crucial to the phosphorylation switch mechanism indicating an extended interaction between TnC and residues 19–34 of TnI. Most of the mutations did alter the  $\text{Ca}^{2+}$  handling properties of the troponin complex, reiterating the functional importance of this region of TnI.

Some of the site-directed mutants used in the stopped flow experiments accelerated  $\text{Ca}^{2+}$  release; however, subsequent phosphorylation was also able to further accelerate  $\text{Ca}^{2+}$  release from these mutants. The stepwise increase in acceleration and the additive effect of the mutations and phosphorylation are most easily explained if the equilibrium between the TnC bound and the TnC unbound states of the phosphorylation switch is very finely poised. The equilibrium can then be perturbed in a graded, rather than all-or-nothing, manner, and even bisphosphorylation does not completely prevent binding (demonstrated by the fact that deleting the N-terminal extension is more effective than phosphorylating it (18) at reducing  $\text{Ca}^{2+}$  affinity). This is seen with the effects of monophosphorylation on  $\text{Ca}^{2+}$  release with each monophosphorylation having approximately half of the effect of bisphosphorylation. Similar stepwise effects of phosphorylation on the affinity of TnI for TnC have been reported (41). Monophosphorylation does not appear to affect  $\text{Ca}^{2+}$  sensitivity in skinned fibers (43) or release the phosphorylation switch from TnC in our HSQC experiments, suggesting that bisphosphorylation is required for physiological effect. Nonetheless, the properties of the monophosphorylated troponin complexes are different from unphosphorylated troponin, and this may be of significance.

Our experiments with –12 TnC provide evidence that it is the N-terminal domain of TnC that the phosphorylation switch interacts with. They also exclude the N-helix of TnC as the primary interaction site for the phosphorylation switch. In the crystal structure of the core domain of troponin (1), the N-helix lies in close proximity to residues 35–44 of TnI. It seemed possible that the N-terminal extension of TnI might bend back and interact with the N-helix; however, this is clearly not the case. The HSQC experiments of Rosevear and co-workers (31, 32) using  $^{15}\text{N}$ -TnC show that bisphosphorylation of S22/23 produces backbone amide shifts in both the regulatory  $\text{Ca}^{2+}$  binding site (site II) and the defunct  $\text{Ca}^{2+}$  site I. This indicates that the phosphorylation switch might bind to site I, although a direct interaction with the regulatory site (or both sites) cannot be excluded. Consistent with the phosphorylation switch possibly binding to site I is the fact that the E76A mutation, preventing  $\text{Ca}^{2+}$  binding at site II, does not have a major effect on the interaction. The effects of this mutation should be localized to site II and not cause major changes in the open-closed equilibrium of the N-terminal domain of TnC in the absence of the regulatory region of TnI (44). Further mutagenesis studies on TnC are required to unequivocally determine where the phosphorylation switch binds.

We find that bisphosphorylation of S41 and S43 of I1–64 by PKC produces only a small reduction in the affinity of I1–64 for TnC in the absence of  $\text{Ca}^{2+}$  and no decrease in the presence of  $\text{Ca}^{2+}$ . This is consistent with recent NMR titrations of  $\text{Ca}^{2+}$  saturated TnC with a peptide corresponding to residues 34–71 of TnI that produced a  $K_D$  of  $\leq 1 \mu\text{M}$  regardless of S41/43 phosphorylation (45). The small decrease in affinity does not involve an alteration in the interaction between the phosphorylation switch and TnC as seen in the experiment of Figure 3. S41 and S43 are at the N-terminus of the helix that binds tightly to the C-terminal domain of TnC. The amide group signals of S41 and S43 are affected by TnC binding, but the side chains do not interact directly with TnC in the core domain crystal structure

(1). The reduction in affinity could arise from conformational changes conducted in the C-terminal direction along the helix to residues involved in binding to the C-terminal domain of TnC or in the N-terminal direction to the phosphorylation switch. The latter mechanism does not seem to occur as our NMR data show that S41/43 bisphosphorylation does not influence the binding of the phosphorylation switch to TnC. We conclude that PKC bisphosphorylation modulates  $\text{Ca}^{2+}$  sensitivity by a quite different mechanism to PKA bisphosphorylation of S22/23. Interestingly, we find that PKC $\alpha$  phosphorylates S22 and S23 of I1–64, as has been shown for a peptide corresponding to residues 17–30 of TnI (46), although it has been reported that PKC $\alpha$  does not phosphorylate S22 and S23 in intact TnI (46). We also demonstrate that PKC $\alpha$  can tetra-kisphosphorylate I1–64, indicating that there is no mutual exclusivity between the two sets of phosphorylation sites (S22/23 and S41/43).

Keane et al. (39) have previously shown that a synthetic peptide corresponding to residues 16–29 binds with a low affinity to TnC and that bisphosphorylation weakens this binding  $\geq 100$ -fold. Ferrieres et al. (47) used an array of immobilized 20mer synthetic peptides to delineate a phosphorylation sensitive TnC binding spanning residues 18–31 of TnI (in very close agreement with our data). We have recently used cross-linking and  $^1\text{H}$  NMR (9, 34) to demonstrate that this interaction also occurs in a more intact system with the N-terminal extension of I1–64 orientated correctly with respect to TnC. The results presented here confirm that the region of the N-terminal extension of TnI around and C-terminal to S22 and S23 binds to the N-terminal domain of TnC in a phosphorylation-sensitive manner. We have also delineated the residues of TnI that are involved in the phosphorylation switch in a functional binary troponin complex for the first time.

## REFERENCES

1. Takeda, S., Yamashita, A., Maeda, K., and Maeda, Y. (2003) Structure of the core domain of human cardiac troponin in the  $\text{Ca}^{2+}$  saturated form, *Nature* 424, 35–41.
2. Perry, S. V. (1998) Troponin T: genetics, properties, and function, *J. Muscle Res. Cell Motil.* 19, 575–602.
3. Herzberg, O., and James, M. N. G. (1985) Structure of the calcium regulatory muscle protein troponin-C at 2.8 Å resolution, *Nature* 313, 653–659.
4. Perry, S. V. (1999) Troponin I: Inhibitor or facilitator, *Mol. Cell. Biochem.* 190, 9–32.
5. Syska, H., Wilkinson, J. M., and Perry, S. V. (1976) The relationship between biological activity and primary structure of troponin I from white skeletal muscle of the rabbit, *Biochem. J.* 153, 375–387.
6. Van Eyk, J. E., Strauss, A. W., Hodges, R. S., and Ruegg, J. C. (1993) A synthetic peptide mimics troponin I function in the calcium-dependent regulation of muscle contraction, *FEBS Lett.* 323, 223–228.
7. Wang, X., Li, M. X., and Sykes, B. D. (2002) Structure of the regulatory N-domain of human cardiac troponin in complex with human cardiac troponin I 147–163 and bepridil, *J. Biol. Chem.* 277, 31124–31133.
8. Vassilyev, D. G., Takeda, S., Wakatsuki, S., Maeda, K., and Maeda, Y. (1998) Crystal structure of troponin C in complex with troponin I fragment at 2.3 Å resolution, *Proc. Natl. Acad. Sci.* 95, 4847–4852.
9. Ward, D. G., Brewer, S. M., Cornes, M. P., and Trayer, I. P. (2003) A cross-linking study of the N-terminal extension of human cardiac troponin I, *Biochemistry* 42, 10324–10332.
10. Stefancsik, R., Jha, P. K., and Sarkar, S. (1998) Identification and mutagenesis of a highly conserved domain in troponin T responsible for troponin I binding: Potential role for coiled coil interaction, *Proc. Natl. Acad. Sci.* 95, 957–962.
11. Ray, K. P., and England, P. J. (1976) Phosphorylation of the inhibitory subunit of troponin and its effect on the calcium dependence of cardiac myofibril adenosine triphosphatase, *FEBS Lett.* 70, 11–16.
12. Solaro, R. J., Moir, A. J. G., and Perry, S. V. (1976) Phosphorylation of troponin I and the inotropic effect of adrenaline in the perfused rabbit heart, *Nature* 262, 615–616.
13. Mittmann, K., Jaquet, K., and Heilmeyer, L. M. G. (1990) A common motif of two adjacent phosphoserines in bovine, rabbit, and human cardiac troponin I, *FEBS Lett.* 273, 41–45.
14. Mittmann, K., Jaquet, K., and Heilmeyer, L. M. G. (1992) Ordered phosphorylation of a duplicated minimal recognition motif for cAMP-dependent protein kinase present in cardiac troponin I, *FEBS Lett.* 302, 133–137.
15. Dohet, C., Al-Hillawi, E., Trayer, I. P., and Ruegg, J. C. (1995) Reconstitution of skinned cardiac fibres with human recombinant cardiac troponin-I mutants and troponin-C, *FEBS Lett.* 377, 131–134.
16. Holroyde, M. J., Howe, E., and Solaro, R. J. (1979) Modification of calcium requirements for activation of cardiac myofibrillar ATPase by cyclic AMP dependent phosphorylation, *Biochim. Biophys. Acta* 586, 63–69.
17. Robertson, S. P., Johnson, D. J., Holroyde, M. J., Kranias, E. G., Potter, J. D., and Solaro, R. J. (1982) The effect of troponin I phosphorylation on the  $\text{Ca}^{2+}$  binding properties of the  $\text{Ca}^{2+}$  regulatory site of bovine cardiac troponin, *J. Biol. Chem.* 257, 260–263.
18. Ward, D. G., Cornes, M. P., and Trayer, I. P. (2002) Structural consequences of cardiac troponin I phosphorylation, *J. Biol. Chem.* 277, 41795–41801.
19. Kentish, J. C., McCloskey, D. T., Layland, J., Palmer, S., Leiden, J. M., Martin, A. F., and Solaro, R. J. (2001) Phosphorylation of troponin I by protein kinase A accelerates relaxation and cross-bridge cycle kinetics in mouse ventricular muscle, *Circ. Res.* 88, 1059–1065.
20. Turnbull, L., Hoh, J. H. Y., Ludowyke, R. I., and Rossmanith, G. H. (2002) Troponin I phosphorylation enhances crossbridge kinetics during  $\beta$ -adrenergic stimulation in rat cardiac tissue, *J. Physiol* 542, 911–920.
21. Noland, T. A., Raynor, R. L., and Kuo, J. F. (1989) Identification of sites phosphorylated in bovine cardiac troponin I and troponin T by protein kinase C and comparative substrate activity of synthetic peptides containing the phosphorylation sites, *J. Biol. Chem.* 264, 20778–20785.
22. Pyle, W. G., Sumandea, M. P., Solaro, R. J., and de Tombe, P. P. (2002) Troponin I serines 43/45 and regulation of cardiac myofilament function, *Am. J. Physiol. Heart. Circ. Physiol.* 283, H1215–H1224.
23. Westfall, M. V., and Borton, A. R. (2003) Role of troponin I phosphorylation in protein kinase C-mediated enhanced contractile performance of rat myocytes, *J. Biol. Chem.* 278, 33694–33700.
24. Burkhart, E. M., Sumandea, M. P., Kobayashi, T., Nili, M., Martin, A. F., Homsher, E., and Solaro, R. J. (2003) Phosphorylation or glutamic acid substitution at protein kinase C sites on cardiac troponin I differentially depress myofilament tension and shortening velocity, *J. Biol. Chem.* 278, 11265–11272.
25. Noland, T. A., Guo, X., Raynor, R. L., Jideama, N. M., Averyhart-Fullard, V., Solaro, J. R., and Kuo, J. F. (1995) Cardiac troponin I mutants. Phosphorylation by protein kinases C and A and regulation of calcium-stimulated MgATPase of reconstituted actomyosin S-1, *J. Biol. Chem.* 270, 25445–25454.
26. Noland, T. A., Raynor, R. L., Jideama, N. M., Guo, X., Kazanietz, M. G., Blumberg, P. M., Solaro, R. J., and Kuo, J. F. (1996) Differential regulation of cardiac actomyosin S1-MgATPase by protein kinase C isozyme-specific phosphorylation of specific sites in cardiac troponin I and its phosphorylation site mutants, *Biochemistry* 35, 14923–14931.
27. Liao, R., Wang, C.-K., and Cheung, H. C. (1992) Time-resolved tryptophan emission study of cardiac troponin I, *Biophys. J.* 63, 986–995.
28. Heller, W. T., Finley, N., Dong, W., Timmins, P., Cheung, H. C., Rosevear, P. R., and Trewhella, J. (2003) Small-angle neutron scattering with contrast variation reveals spatial relationships between the three subunits in the ternary cardiac troponin complex and the effects of troponin I phosphorylation, *Biochemistry* 42, 7790–7800.

29. Dong, W.-J., Chandra, M., Xing, J., She, M., Solaro, R. J., and Cheung, H. C. (1997) Phosphorylation-induced distance change in a cardiac muscle troponin I mutant, *Biochemistry* 36, 6754–6761.
30. Abbot, M. B., Gaponenko, V., Abusamhadneh, E., Finley, N., Li, G., Dvoretzky, A., Rance, M., Solaro, R. J., and Rosevear, P. R. (2000) Regulatory domain conformational exchange and linker region flexibility in cardiac troponin C bound to cardiac troponin I, *J. Biol. Chem.* 275, 20610–20617.
31. Finley, N., Abbot, M. B., Abusamhadneh, E., Gaponenko, V., Dong, W.-J., Gasmi-Seabrook, G., Howarth, J. W., Rance, M., Solaro, R. J., Cheung, H. C., and Rosevear, P. R. (1999) NMR analysis of cardiac troponin C-troponin I complexes: effects of phosphorylation, *FEBS Lett.* 453, 107–112.
32. Gaponenko, V., Abusamhadneh, E., Abbot, M. B., Finley, N., Gasmi-Seabrook, G., Solaro, R. J., Rance, M., and Rosevear, P. R. (1999) Effects of troponin I phosphorylation on conformational exchange in the regulatory domain of cardiac troponin C, *J. Biol. Chem.* 274, 16681–16684.
33. Chandra, M., Dong, W.-J., Pan, B.-S., Cheung, H. C., and Solaro, R. J. (1997) Effects of protein kinase A phosphorylation on signaling between cardiac troponin I and the N-terminal domain of cardiac troponin C, *Biochemistry* 36, 13305–13311.
34. Ward, D. G., Brewer, S. M., Calvert, M. J., Gallon, C. E., Gao, Y., and Trayer, I. P. (2004) Characterization of the interaction between the N-terminal extension of cardiac TnI and TnC, *Biochemistry* 43, 4020–4027.
35. Al-Hillawi, E., Minchin, S. D., and Trayer, I. P. (1994) Overexpression of human cardiac troponin I and troponin C in *Escherichia coli* and their purification and characterization, *Eur. J. Biochem.* 225, 1195–1201.
36. Hahn, E. L. (1950) Spin-echoes, *Phys. Rev.* 80, 580–594.
37. Campbell, I. D., Dobson, C. M., Williams, R. J. P., and Wright, P. E. (1975) Pulse methods for the simplification of protein NMR spectra, *FEBS Lett.* 57, 96–99.
38. Abbot, M. B., Dong, W.-J., Dvoretzky, A., DaGue, B., Caprioli, R. M., Cheung, H. C., and Rosevear, P. R. (2001) Modulation of cardiac troponin C-cardiac troponin I regulatory interactions by the amino-terminus of cardiac troponin I, *Biochemistry* 40, 5992–6001.
39. Keane, N. E., Quirke, P. G., Gao, Y., Patchell, V. B., Perry, S. V., and Levine, B. A. (1997) The ordered phosphorylation of cardiac troponin I by the cAMP-dependent protein kinase, *Eur. J. Biochem.* 248, 329–337.
40. Reiffert, S., Maytum, R., Geeves, M. A., Lohmann, K., Greis, T., Bluggel, M., Meyer, H. E., Heilmeyer, L. M. G., and Jaquet, K. (1999) Characterization of the cardiac holotroponin complex reconstituted from native cardiac troponin T and recombinant I and C, *Eur. J. Biochem.* 261, 40–47.
41. Reiffert, S., Jaquet, K., Heilmeyer, L. M. G., and Herberg, F. W. (1998) Stepwise subunit interaction changes by mono- and bisphosphorylation of cardiac troponin I, *Biochemistry* 37, 13516–13525.
42. Jaquet, K., Lohmann, K., Czisch, M., Holak, T., Gulati, J., and Jaquet, R. (1998) A model for the function of the bisphosphorylated heart-specific troponin-I N-terminus, *J. Muscle Res. Cell Motil.* 19, 647–659.
43. Zhang, R., Zhao, J. J., and Potter, J. D. (1995) Phosphorylation of both serine residues in cardiac troponin is required to decrease the Ca<sup>2+</sup> affinity of cardiac troponin-C, *J. Biol. Chem.* 270, 30773–30780.
44. Sia, S. K., Li, M. X., Spyropoulos, L., Gagne, S. M., Liu, W., Putkey, J. A., and Sykes, B. D. (1997) Structure of cardiac muscle troponin C unexpectedly reveals a closed regulatory domain, *J. Biol. Chem.* 272, 18216–18221.
45. Li, M. X., Wang, X., Lindhout, D. A., Buscemi, N., Van Eyk, J. E., and Sykes, B. D. (2003) Phosphorylation and mutation of human cardiac troponin I differentially destabilize the interaction of the functional regions of troponin I with troponin C, *Biochemistry* 42, 14460–14468.
46. Jideama, N. M., Noland, T. A., Raynor, R. L., Blobe, G. C., Fabbro, D., Kazanietz, M. G., Blumberg, P. M., Hannun, Y. A., and Kuo, J. F. (1996) Phosphorylation specificities of protein kinase C isozymes for bovine cardiac troponin I and troponin T and sites within these proteins and regulation of myofilament properties, *J. Biol. Chem.* 271, 23277–23283.
47. Ferrieres, G., Pugniere, M., Mani, J. C., Villard, S., Laprade, M., Dautre, P., Pau, B., and Granier, C. (2000) Systematic mapping of regions of human cardiac troponin I involved in binding to cardiac troponin C: N- and C-terminal low affinity contributing regions, *FEBS Lett.* 479, 99–105.

BI036310M